Proceedings of ISFOG 2025
5TH INTERNATIONAL SYMPOSIUM ON
FRONTIERS IN OFFSHORE GEOTECHNICS
Nantes, France | June 9-13 2025

ISBN 978-2-85782-758-0

Experimental Study of the Effects of Cyclic Loading on Base Resistance Mobilization of Piles Using a Calibration Chamber

A. C. Galvis-Castro*
Norwegian Geotechnical Institute, Houston, TX, USA

R. D. Tovar-Valencia
Fugro, Houston, TX, USA

M. Prezzi, R. Salgado
Lyles School of Civil Engineering, Purdue Univ., West Lafayette, IN, USA
* *ayda.galvis@ngi.no*

ABSTRACT: Cyclic loading significantly changes soil behaviour, particularly in structures such as piles. In this paper, the results of a series of monotonic compressive and cyclic load tests on a jacked closed-ended model pile are presented. Notable findings of this work include a reduction in ultimate unit base resistance following cyclic loading. Interestingly, large cycling displacement amplitude leads to increased limit unit base resistance. This phenomenon results from sand particle movement, particle crushing, and sand dilatancy. Additionally, Digital Image Correlation (DIC) analysis of pictures taken during the tests revealed that, for cyclic displacement half amplitudes of 0.25 mm or less, normalized cumulative radial and vertical displacements in the soil remain minimal. Beyond this threshold, residual displacements increase with increasing cyclic amplitude. The understanding of load cycling effects is crucial for designing resilient geotechnical structures, such as plugged jacket piles for offshore platform.

Keywords: Piles; cyclic; loading; sand; DIC.

1. INTRODUCTION

Cyclic loading can significantly change soil behaviour, which in turn affects the performance of geotechnical structures such as the foundation for offshore platforms. These structures often experience load reversals from environmental factors like wind and waves, leading to degradation of soil resistance, especially in offshore foundations (Bhattacharya et al., 2017; Liu et al., 2023). For piles subjected to cyclic loading, such as those used to support offshore platforms, the impact on pile base resistance and overall structural response is a critical consideration.

Several methods, such as the boundary-element method and load-transfer method, are used to analyse cyclic loading on piles (Poulos 1989; Randolph and Jewell 1989). These methods rely on empirical criteria to model soil-pile interaction and predict cyclic loading effects, including capacity degradation and permanent displacement. However, limited experimental data are available to validate predictions for base resistance under cyclic loading conditions (Galvis-Castro et al., 2023; Puech 2013; Stuyts et al., 2012).

Experimental studies, model pile testing and soil-structure interface element testing indicate that the pile response to cyclic loading is influenced by cycle count, load type, and amplitude (Jardine and Standing 2012; Tsuha et al., 2012) as well as soil-surface interaction e.g., normalized roughness (Westgate et al., 2023). Changes in pile response result from changes in soil state—including density and fabric—around the pile, which can be studied using Digital image correlation (DIC). DIC has emerged as a useful tool in geotechnical modelling, allowing for the analysis of soil deformation around piles under cyclic loads (Doreau-Malioche et al., 2018).

This study presents results from cyclic and monotonic load tests on a jacked model pile in a calibration chamber, focusing on the effects of cyclic displacement amplitude and cycle number on base resistance, along with insights into soil displacement mechanisms.

2. MATERIALS AND METHODS

The tests discussed in this paper were conducted in a half-cylindrical steel calibration chamber with an internal diameter of 1680 mm and a height of 1200 mm. The front wall of the chamber is made of Plexiglass, reinforced with a steel frame, enabling digital imaging of the model pile and surrounding soil during installation and loading. Further details of the chamber are provided by (Arshad et al., 2014) and (Tovar-Valencia et al., 2022).

The model pile is a half-circular rod with diameter B = 38.1. A conical base with a 60 degrees apex angle is attached to its base. The load at the pile head was measured using a specially designed tension/compression load cell with a rated capacity of 42 kN. Additionally, four electrical-resistance strain gauges were placed diametrically opposed to each other in a cylindrical brass rod at the tip (see Figure 1) to measure the axial deformation and determine the load at the base of the model pile. A schematic of the setup and equipment is shown in Figure 1.

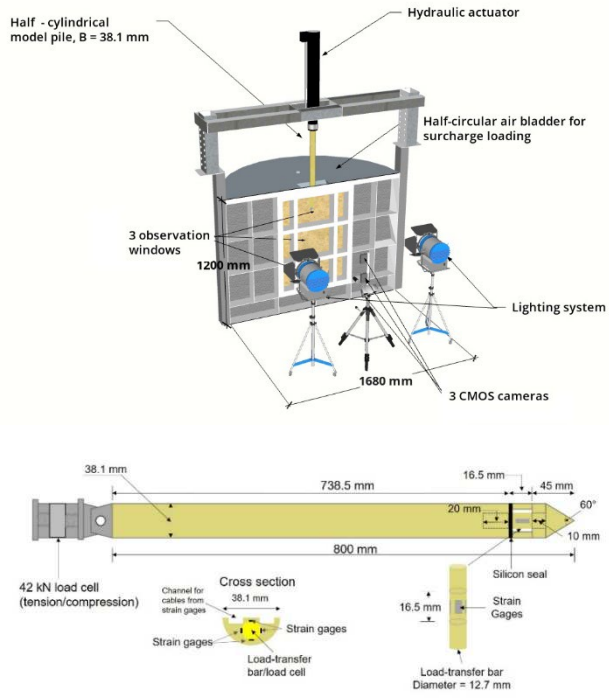

Figure 1. Schematic of calibration chamber and model pile (model pile diameter B = 38.1 mm)

The experimental sand used was Ohio Gold Frac, a poorly graded silica sand. Its mean particle size (D_{50}) is 0.62 mm with a coefficient of uniformity (C_U) of 1.46. The sand particles, which ranged from sub-angular to sub-rounded, had an average roundness of 0.51 (Wadell, 1932).

3. EXPERIMENTAL PROCEDURE

Three model pile tests were performed within a half-cylindrical calibration chamber filled with dry silica sand. All the tests were performed in dry conditions.

The tests were conducted the following sequence of steps:

a) Soil sample preparation: The samples were prepared by air pluviation using a large-scale pluviator placed above the calibration chamber to ensure consistent sample density (Lee et al., 2011).
b) Cameras and load system setup: Once the sand sample was prepared, the loading system and cameras were positioned in front of the chamber (see Figure 1).
c) Surcharge: A surcharge was applied at the top of the sample. This involved using a rubber bladder and a reaction steel lid bolted to the chamber. The surcharge resulted in an initial vertical effective stress of 33 kPa at the level of the pile base. This value was measured in additional tests not reported in this paper with the same sand density and boundary conditions.
d) Pile jacking: The model pile was installed using jacking strokes of 10 mm at a controlled rate of 1.0 mm/s.
e) End of installation: The final installation depth was 415 mm (= 10.9B). Once the model pile base reached the desired penetration depth, it was unloaded. This step simulated the end of the installation process.
f) Monotonic load test before cycling: Following the installation, a compressive load was applied by pushing the model pile downward at a constant rate of 0.1 mm/s. The displacement covered approximately 12 mm (0.3B).
g) Unloading: The pile was unloaded by detaching the loading system from the model pile head.
h) Preloading: The pile was then loaded monotonically until it reached a base settlement w_b of 0.01B. This settlement corresponded to an approximate unit base resistance of 28% relative to the limit unit base resistance $q_{bL,BC}$, measured before cyclic loading. The limit unit base resistance q_{bL} corresponds to the limiting value of the unit base load at which the soil mass surrounding the pile can no longer generate additional resistance, leading to plunging of pile (Bansu and Salgado, 2012). The value of $q_{bL,BC}$ is obtained from the monotonic load test described in (f).
i) Cyclic loading: Displacement-controlled cycles were applied to the head of the pile. These cycles

involved uniform sinusoidal displacement with half-amplitude (Δw_{cyclic}) ranging from 0.25 mm ($0.007B = 0.4D_{50}$) to 3.0 mm ($0.079B = 4.8\ D_{50}$). The tests were performed with 100 cycles (N_c) using a frequency of 0.1 Hz.

j) Unloading: After completing the cyclic stage, any remaining load from the model pile head was removed by disconnecting the load system from the head of the model pile.

k) Monotonic load test after cycling: In the final test phase, the model pile was loaded in compression under displacement-controlled conditions to a depth of at least 1B at a rate of 0.1 mm/s.

Table 1 shows the test matrix and details of the cyclic loads applied.

Table 1. Testing program.

Test code[a,b]	Relative density D_R (%)	Cyclic displacement half amplitude Δw_{cyclic} (mm)	Number of cycles N_c	Frequency f (Hz)
CY3.0-N100	93.0	3.00	100	0.1
CY1.0-N100	88.2	1.00	100	0.1
CY0.25-N100	91.3	0.25	100	0.1

[a] Test code: CY'#'= cyclic displacement half amplitude Δw_{cyclic} followed by its value in mm, N'#' = number of cycles.
[b] The model pile was installed by jacking strokes of 10 mm length. A initial vertical effective stress σ_0' of 33 kPa at the level of the pile base was applied in all tests.

The digital images captured during the tests were analysed using the Digital Image Correlation (DIC) technique to determine the vertical and radial displacement in the sand around the model pile base during cyclic loading. The commercial software VIC-2D (Correlated Solutions 2009) was utilized for DIC analysis. The settings and fundamentals of the DIC technique are detailed in Galvis-Castro et al. (2023).

The vertical and radial displacements in the sand domain surrounding the model pile base during cyclic loading obtained from the DIC analyses were interpolated using the Kriging method to generate contour lines for both radial and vertical displacements.

For comparison, the digital images obtained at the end of the cycling stage of tests CY0.25-N100 and CY3.0-N100 are shown in Figure 2. It is observed that the zone of crushed particles (crushed particles are lightly coloured) near the pile base is significantly smaller than that for test CY3.0-N100. The area of crushed particles induced by the cyclic loading forms a bulb below the tip of the cone that extends vertically to a distance, measured from the tip, of approximately 0.4B for tests CY3.0-N100.

Although grain size distribution (GSD) and the relative breakage parameter were not determined directly in these tests, images revel changes in GSD. Further details about particle crushing around the conical tip after cyclic loading are provided in Galvis-Castro et al. (2023). In addition, experimental investigation on the particle gradation changes around the conical base of model piles during installation and monotonic loading for similar model pile test settings, as those presented in this paper, are provided in Tovar-Valencia et al. (2022) and Ganju et al. (2022).

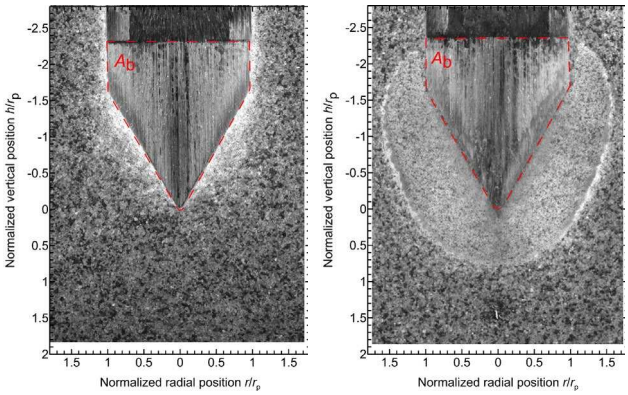

(a) *(b)*

Figure 2. Digital images at the end of the cycling stage of tests: (a) CY0.25-N100 and (b) CY3.0-N100

4. ANALYSIS OF RESULTS

4.1. Effect of cyclic loading on base resistance

Figure 3 shows the measured unit base resistance (q_b) versus relative settlement (w_b/B) at the pile base for compressive load tests conducted before and after the cyclic loading stage of tests CY0.25-N100, CY1.0-N100, and CY3.0-N100. The tests differ only in their cyclic displacement half-amplitude (Δw_{cyclic}) values, which were set at of 0.25 mm, 0.5 mm, 1.0 mm, and 1.5 mm.

Figure 3 shows that, for $\Delta w_{cyclic} = 0.25$ mm, the base resistance measured before and after cyclic loading did not change. For $\Delta w_{cyclic} = 1.0$ mm the results show that, at low values w_b/B (< 0.1), the difference in base resistance can be as high as 60%; however, the difference between $q_{b,AC}$, and $q_{b,BC}$ decreases as w_b/B increases. Figure 3 shows that, for the highest analysed cyclic displacement (Δw_{cyclic}=3.0 mm), the base resistance measured after cycling is less than that measured before cyclic loading for normalized base displacements w_b/B<0.3. When w_b/B exceeds 0.3, $q_{b,AC}$ increases with relative settlement to as much as 140% of the limit unit base resistance (14.4 MPa) measured before cycling. The lower unit base resistance for w_b/B<0.3 suggests that the crushed material seen in Figure 2b, which surrounds the conical base is less dense than that before cycling. As the conical pile base passes the bulb of crushed sand particles, it goes through densified sand with dilative tendency,

resulting in higher unit base resistance (Galvis-Castro et al., 2023).

From Figure 3, it can be inferred that the tangent stiffness (i.e., ratio of Δq_b to Δw_b) in the monotonic compressive load performed after cyclic loading is lower than that before cyclic loading. After cyclic loading, the tangent stiffness measured at t $w_b = 0.05B$ reduced by about 50 % and 25% for test CY1.0-N100 and CY3.0-N100, respectively. For $w_b > 0.1B$, a local flow of particles from the region above the shoulder of the conical base into the gap created during the pull-out stage of each cycle occurs in test CY3.0-N100. This flow of particles beneath the tip of the cone may explain the slightly higher stiffness observed in test CY3.0-N100 after cyclic loading compared to test CY1.0-N100 at the same stage.

4.2. Effect of cyclic loading on soil displacement

Figure 4 presents the contours lines of normalized cumulative radial displacement $u/\Delta w_{cyclic}$ at the end of cycling stage of tests CY0.25-N100, CY1.0-N100, and CY3.0-N100. Figure 5 presents the contours lines of normalized cumulative vertical displacement $v/\Delta w_{cyclic}$ at the end of cycling stage of tests CY0.25-N100, CY1.0-N100, and CY3.0-N100. The cumulative radial displacement u and cumulative vertical displacement v were normalized by the value of the cyclic displacement half amplitude Δw_{cyclic} of the corresponding test and plotted at the original undeformed locations of the soil elements. In these figures, the x-axis corresponds to the horizontal distance r from the centreline of the model pile to the soil element, normalized by the model pile radius r_p; and the y-axis corresponds to the vertical distance h of a soil element with respect to the pile base ($h = 0$ at the pile base, positive above it, and negative below it), also normalized by the model pile radius r_p.

In Figure 4, the value of $u/\Delta w_{cyclic}$ was added on top of the corresponding contour lines, when possible. Positive values of $u/\Delta w_{cyclic}$ indicate the soil elements moved away from the centreline of the model pile and negative values of $u/\Delta w_{cyclic}$ indicate the soil elements moved towards it after cyclic loading. In Figure 5, positive values of $v/\Delta w_{cyclic}$ indicate the soil elements moved upward and negative values indicate they moved downward after cyclic loading.

Figure 4 and Figure 5 indicate that, for a cyclic displacement half amplitude Δw_{cyclic} of 0.25 mm, the normalized radial and vertical displacements accumulated around the conical base after cyclic loading remain negligible after 100 cycles, being smaller than 0.05. For $\Delta w_{cyclic} = 1.0$ mm, soil elements under the conical base exhibit positive cumulative radial displacement greater than $0.1\Delta w_{cyclic}$ and negative cumulative vertical displacement less than $-0.1\Delta w_{cyclic}$, causing them to move radially outward and downward. In contrast, at the conical base shoulder, soil elements display negative cumulative radial displacement less than $-0.1\Delta w_{cyclic}$ and positive cumulative vertical displacement greater than $0.1\Delta w_{cyclic}$, indicating that soil elements move radially away from the pile axis and downward. For test CY3.0-N100, there is a region close to the cone shoulder where the DIC analysis did not produce any information. This is due mainly to the large displacements and rotations of the soil particles located next to the shoulder of the conical base during cycling, causing the DIC algorithm to fail tracking these soil elements (Tovar-Valencia et al., 2022). When data is available, Figure 4(c) and Figure 5(c) show that the soil elements move considerably more in comparison with tests with Δw_{cyclic} of 0.25 mm and 1.0 mm. The results shown in Figure 4(c) indicate that soil elements with normalized radial displacements $u/\Delta w_{cyclic}$ greater than 0.1 extend to a radial position r/r_p equal to 4 and a vertical distance h/r_p of -3.0. Similarly, in Figure 5(c) the cumulative vertical displacements of soil elements initially positioned between h/r_p of -3.0 and 0 move downward more than 20% the value of the Δw_{cyclic} (= 3.0 mm).

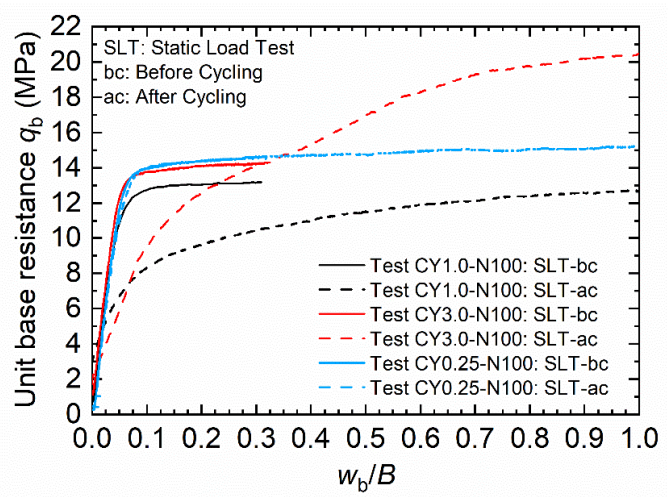

Figure 3. Unit base resistance q_b mobilized in the compressive load tests performed before and after cycling versus relative settlement w_b/B at the pile base

5. CONCLUSIONS

This paper presents the results of monotonic and cyclic load tests on a closed-ended jacked model pile with a conical base. The tests were performed in dense silica sand, and images taken during the tests were analysed to measure displacement and strain fields around the conical base. Although the behaviour of

closed-ended piles differs from that of open-ended piles, the results of these tests can reflect conditions in which a plug forms inside open-ended piles in certain conditions.

Cyclic loading with a half-amplitude Δw_{cyclic} of 0.25 mm showed minimal effect on unit base resistance, whereas tests with Δw_{cyclic} of 1.0 mm resulted in a reduction of unit base resistance following cyclic loading. In contrast, tests with Δw_{cyclic} of 3.0 mm initially reduced base resistance but ultimately led to an increase in resistance after the pile base displacement reached 1*B*. DIC results indicated minor disturbance to soil near the conical base during such loading. In contrast, tests performed with Δw_{cyclic} = 1.0 mm showed that, after 100 cycles, the ultimate unit base resistance at w_b/B=0.1 significantly decreased as compared with static load tests performed before the cyclic loading. Additionally, cumulative radial and vertical displacements increased when compared with the tests done with Δw_{cyclic} = 0.25mm.

Tests performed with Δw_{cyclic} = 3.0 mm showed that the ultimate unit base resistance measured after cyclic loading increases with relative settlement when w_b/B > 0.3, being up to 40% greater than the limit unit base resistance (14.4 MPa) measured before cycling.

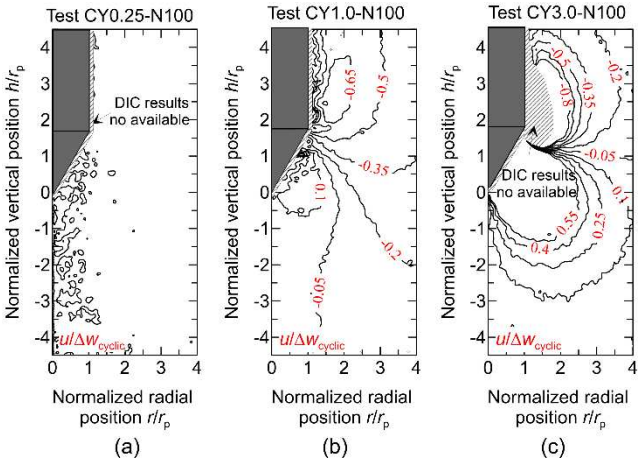

Figure 4. Contours of normalized radial displacement $u/\Delta w_{cyclic}$ (positive when soil moves away from the model pile centreline) near the conical base after 100 cycles with cyclic displacement half amplitude Δw_{cyclic} of (a) 0.25 mm, (b) 1.0 mm, and (c) 3.0 mm

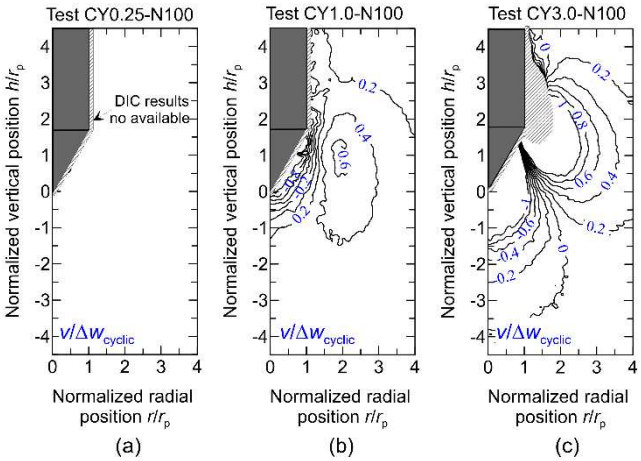

Figure 5. Contours of normalized vertical displacement $v/\Delta_{wcyclic}$ (positive when soil elements move upward) near the conical base after 100 cycles with cyclic displacement half amplitude Δw_{cyclic} of (a) 0.25 mm, (b) 1.0 mm, and (c) 3.0 mm

AUTHOR CONTRIBUTION STATEMENT

A. C. Galvis-Castro: Testing, Formal Analysis, Writing- Original Draft. **R. D. Tovar-Valencia**: Testing, Writing- Reviewing, Conceptualization. **M. Prezzi & R. Salgado**: Supervision, Funding Acquisition, Writing- Reviewing and Editing.

REFERENCES

Arshad, M., F. Tehrani, M. Prezzi, and R. Salgado. 2014. "Experimental study of cone penetration in silica sand using digital image correlation." *Geotechnique*, 64 (7): 551–569.

Bhattacharya, S., G. Nikitas, L. Arany, and N. Nikitas. 2017. "Soil–Structure Interactions for Offshore Wind Turbines." *Engineering & Technology Reference*, 1 (1): 1–16. https://doi.org/10.1049/etr.2016.0019.

Basu, D., and Salgado, R. (2012). "Load and resistance factor design of drilled shafts in sand." *Journal of Geotechnical and Geoenvironmental Engineering*, 138(12), 1455–1469.

Correlated Solutions. 2009. *VIC-2D [computer software]. Reference manual*. Columbia, SC, USA: Correlated Solutions.

Doreau-Malioche, J., G. Combe, G. Viggiani, and J. B. Toni. 2018. "Shaft friction changes for cyclically loaded displacement piles: an X-ray investigation." *Géotechnique Letters*, 8: 66–72. https://doi.org/10.1680/jgele.17.00141.

Galvis-Castro, A. C., R. D. Tovar-Valencia, M. Prezzi, and R. Salgado. 2023. "Effect of cyclic loading on the mobilization of unit base resistance of model piles jacked in sand." *Acta Geotechnica, 18(9),* 4747-4766. https://doi.org/10.1007/s11440-023-01840-5.

Ganju, E., Han, F., Prezzi, M., Salgado, R., and Pereira, J. S. 2020. "Quantification of displacement and particle crushing around a penetrometer tip." *Geoscience Frontiers*, 11(2), 389-399. https://doi.org/10.1016/j.gsf.2019.05.007

Jardine, R. J., and J. R. Standing. 2012. "Field axial cyclic loading experiments on piles driven in sand." *Soils and Foundations*, 52 (4): 723–736. Elsevier. https://doi.org/10.1016/j.sandf.2012.07.012.

Liu, C., C. Yan, G. Zheng, T. Liu, and Y. Yang. 2023. "Field Testing and Numerical Analysis of Supporting Performance of Oblique Piles Used in Pit Excavation." *International Journal of Geomechanics*, 23 (11): 04023204. American Society of Civil Engineers. https://doi.org/10.1061/IJGNAI.GMENG-8487.

Poulos, H. G. 1989. "Cyclic Axial Loading Analysis of Piles in Sand." *Journal of Geotechnical Engineering*, 115 (6): 836–852.

Puech, A. 2013. "Advances in axial cyclic pile design: Contribution of the SOLCYP project." *ISSMGE Technical Committee TC 209 – Offshore Geotechnics*, 45–57.

Randolph, M. F., and R. J. Jewell. 1989. "Load transfer model for pile in calcareous soil." *International Conference on Soil Mechanics and Foundation Engineering, 12th*, 479–484. Rio De Janeiro: Rotterdam, Netherlands.

Stuyts, B., D. Cathie, H. Falepin, and A. Burgraeve. 2012. "Axial pile capacity of wind turbine foundations subject to cyclic loading." *Offshore Site Investigation and Geotechnics 2012: Integrated Technologies - Present and Future, OSIG 2012*, 315–322.

Tovar-Valencia, R. D., A. C. Galvis-Castro, R. Salgado, M. Prezzi, and D. Fridman. 2022. "Experimental measurement of particle crushing around model piles jacked in a calibration chamber." *Acta Geotechnica*, 1–21. https://doi.org/10.1007/s11440-022-01681-8.

Tsuha, C. H. C., P. Y. Foray, R. J. Jardine, Z. X. Yang, M. Silva, and S. Rimoy. 2012. "Behaviour of displacement piles in sand under cyclic axial loading." *Soils and Foundations*, 52 (3): 393–410. Elsevier. https://doi.org/10.1016/j.sandf.2012.05.002.

Wadell, H. 1932. "Volume, shape, and roundness of rock particles." *The Journal of Geology*, 40 (5): 443–451.

Westgate, Z. J., & DeJong, J. T. 2023. "Role of Initial State, Material Properties, and Confinement Condition on Local and Global Soil–Structure Interface Behavior during Cyclic Shear." *Journal of Geotechnical and Geoenvironmental Engineering*, 149(10), 04023088.